Physics Letters B 267 (1991) 422–430
North-Holland

PHYSICS LETTERS B

A measurement of the lifetime of the tau lepton

DELPHI Collaboration

P. Abreu [a], W. Adam [b], F. Adami [c], T. Adye [d], T. Akesson [e], G.D. Alekseev [f], P. Allen [g], S. Almehed [e], S.J. Alvsvaag [h], U. Amaldi [i], E. Anassontzis [j], P. Antilogus [k], W.-D. Apel [ℓ], R.-J. Apsimon [d], B. Åsman [m], P. Astier [n], J.-E. Augustin [o], A. Augustinus [i], P. Baillon [i], P. Bambade [o], F. Barao [a], G. Barbiellini [p], D.Y. Bardin [f], A. Baroncelli [q], O. Barring [e], W. Bartl [b], M. Battaglia [r], M.J. Bates [s], M. Baubillier [n], K.-H. Becks [t], C.J. Beeston [s], M. Begalli [u], P. Beilliere [v], Yu. Belokopytov [w], P. Beltran [x], D. Benedic [y], J.M. Benlloch [g], M. Berggren [m], D. Bertrand [z], F. Bianchi [aa], J.H. Bibby [s], M.S. Bilenky [f], P. Billoir [n], J. Bjarne [e], D. Bloch [y], S. Blyth [s], P.N. Bogolubov [f], T. Bolognese [c], M. Bonapart [ab], M. Bonesini [r], W. Bonivento [r], P.S.L. Booth [ac], M. Boratav [n], P. Borgeaud [c], G. Borisov [w], H. Borner [s], C. Bosio [q], B. Bostjancic [i], O. Botner [ad], B. Bouquet [o], M. Bozzo [u], S. Braibant [i], P. Branchini [q], K.D. Brand [ae], R.A. Brenner [af], C. Bricman [z], R.C.A. Brown [i], N. Brummer [ab], J.-M. Brunet [v], L. Bugge [ag], T. Buran [ag], H. Burmeister [i], J.A.M.A. Buytaert [z], M. Caccia [i], M. Calvi [r], A.J. Camacho Rozas [ah], J.-E. Campagne [i], A. Campion [ac], T. Camporesi [i], V. Canale [ai], F. Cao [z], F. Carena [i], L. Carroll [ac], C. Caso [u], E. Castelli [p], M.V. Castillo Gimenez [g], A. Cattai [i], F.R. Cavallo [aj], L. Cerrito [ai], A. Chan [ak], P. Charpentier [i], P. Checchia [ae], G.A. Chelkov [f], L. Chevalier [c], P. Chliapnikov [w], V. Chorowicz [n], R. Cirio [aa], M.P. Clara [aa], P. Collins [s], J.L. Contreras [a,ℓ], R. Contri [u], G. Cosme [o], F. Couchot [o], H.B. Crawley [ak], D. Crennell [d], G. Crosetti [u], N. Crosland [s], M. Crozon [v], J. Cuevas Maestro [ah], S. Czellar [af], S. Dagoret [o], E. Dahl-Jensen [am], B. Dalmagne [o], M. Dam [i], G. Damgaard [am], G. Darbo [u], E. Daubie [z], P.D. Dauncey [s], M. Davenport [i], P. David [n], A. De Angelis [p], M. De Beer [c], H. De Boeck [z], W. De Boer [ℓ], C. De Clercq [z], M.D.M. De Fez Laso [g], N. De Groot [ab], C. De La Vaissiere [n], B. De Lotto [p], A. De Min [r], C. Defoix [v], D. Delikaris [i], S. Delorme [i], P. Delpierre [v], N. Demaria [aa], J. Derkaoui [aa,1], L. Di Ciaccio [ai], H. Dijkstra [i], F. Djama [y], J. Dolbeau [v], M. Donszelmann [ab], K. Doroba [an], M. Dracos [i], J. Drees [t], M. Dris [ao], Y. Dufour [v], W. Dulinski [y], L.-O. Eek [ad], P.A.-M. Eerola [af], T. Ekelof [ad], G. Ekspong [m], A. Elliot Peisert [ae], J.-P. Engel [y], V. Falaleev [w], D. Fassouliotis [ao], M. Fernandez Alonso [ah], A. Ferrer [g], T.A. Filippas [ao], A. Firestone [ak], H. Foeth [i], E. Fokitis [ao], P. Folegati [p], F. Fontanelli [u], K.A.J. Forbes [ac], H. Forsbach [t], B. Franek [d], P. Frenkiel [v], D.C. Fries [ℓ], A.G. Frodesen [h], R. Fruhwirth [b], F. Fulda-Quenzer [o], K. Furnival [ac], H. Furstenau [ℓ], J. Fuster [i], J.M. Gago [a], G. Galeazzi [ae], D. Gamba [aa], C. Garcia [g], J. Garcia [ah], U. Gasparini [ae], P. Gavillet [i], E.N. Gazis [ao], J.-P. Gerber [y], P. Giacomelli [aj], K.-W. Glitza [t], R. Gokieli [i], V.M. Golovatyuk [f], J.J. Gomez Y Cadenas [i], A. Goobar [m], G. Gopal [d], M. Gorski [an], V. Gracco [u], A. Grant [i], F. Grard [z], E. Graziani [q], M.-H. Gros [o], G. Grosdidier [o], E. Gross [i], B. Grossetete [n], S. Gumenyuk [w], J. Guy [d], F. Hahn [i], M. Hahn [ℓ], S. Haider [ab], Z. Hajduk [ab], A. Hakansson [e], A. Hallgren [ad], K. Hamacher [t], G. Hamel De Monchenault [c], F.J. Harris [s], B.W. Heck [i], T. Henkes [i], I. Herbst [t], J.J. Hernandez [g], P. Herquet [z], H. Herr [i], I. Hietanen [af], C.O. Higgins [ac], E. Higon [g], H.J. Hilke [i], S.D. Hodgson [s], T. Hofmokl [an], R. Holmes [ak], S.-O. Holmgren [m], D. Holthuizen [ab], P.F. Honore [v], J.E. Hooper [am], R. Horisberger [i], M. Houlden [ac], J. Hrubec [b], P.O. Hulth [m], K. Hultqvist [m], D. Husson [y], B.D. Hyams [i], P. Ioannou [j], D. Isenhower [i], P.-S. Iversen [h], J.N. Jackson [ac], P. Jalocha [ap], G. Jarlskog [e], P. Jarry [c], B. Jean-Marie [o], E.K. Johansson [m], D. Johnson [ac], M. Jonker [i], L. Jonsson [e], P. Juillot [y], G. Kalkanis [j], G. Kalmus [d],

G. Kantardjian [i], F. Kapusta [n], S. Katsanevas [j], E.C. Katsoufis [ao], R. Keranen [af], J. Kesteman [z], B.A. Khomenko [f], N.N. Khovanski [f], B. King [ac], N.J. Kjaer [am], H. Klein [i], W. Klempt [i], A. Klovning [h], P. Kluit [ab], J.H. Koehne [ℓ], B. Koene [ab], P. Kokkinias [x], M. Kopf [ℓ], M. Koratzinos [i], K. Korcyl [ap], A.V. Korytov [f], B. Korzen [i], V. Kostukhin [w], C. Kourkoumelis [j], T. Kreuzberger [b], J. Krolikowski [an], U. Kruener-Marquis [t], W. Krupinski [ap], W. Kucewicz [r], K. Kurvinen [af], C. Lacasta [g], C. Lambropoulos [x], J.W. Lamsa [ak], L. Lanceri [p], V. Lapin [w], J.-P. Laugier [c], R. Lauhakangas [af], G. Leder [b], F. Ledroit [v], J. Lemonne [z], G. Lenzen [t], V. Lepeltier [o], A. Letessier-Selvon [n], D. Liko [b], E. Lieb [t], E. Lillethun [h], J. Lindgren [af], A. Lipniacka [an], I. Lippi [ae], R. Llosa [aℓ], B. Loerstad [e], M. Lokajicek [f], J.G. Loken [s], M.A. Lopez Aguera [ah], A. Lopez-Fernandez [o], M. Los [ab], D. Loukas [x], A. Lounis [y], J.J. Lozano [g], R. Lucock [d], P. Lutz [v], L. Lyons [s], G. Maehlum [i], J. Maillard [v], A. Maltezos [x], S. Maltezos [ao], F. Mandl [b], J. Marco [ah], M. Margoni [ae], J.-C. Marin [i], A. Markou [x], S. Marti [g], L. Mathis [v], F. Matorras [ah], C. Matteuzzi [r], G. Matthiae [ai], M. Matveev [w], M. Mazzucato [ae], M. Mc Cubbin [ac], R. Mc Nulty [ac], E. Menichetti [aa], G. Meola [u], C. Meroni [r], W.T. Meyer [ak], M. Michelotto [ae], W.A. Mitaroff [b], G.V. Mitselmakher [f], U. Mjoernmark [e], T. Moa [m], R. Moeller [am], K. Moenig [t], M.R. Monge [u], P. Morettini [u], H. Mueller [ℓ], H. Muller [i], W.J. Murray [d], G. Myatt [s], F. Naraghi [n], U. Nau-Korzen [t], F.L. Navarria [aj], P. Negri [r], B.S. Nielsen [am], B. Nijjhar [ac], V. Nikolaenko [w], V. Obraztsov [w], A.G. Olshevski [f], R. Orava [af], A. Ostankov [w], A. Ouraou [c], R. Pain [n], H. Palka [ab], T. Papadopoulou [ao], L. Pape [i], A. Passeri [q], M. Pegoraro [ae], V. Perevozchikov [w], M. Pernicka [b], A. Perrotta [aj], F. Pierre [c], M. Pimenta [a], O. Pingot [z], A. Pinsent [s], M.E. Pol [a], G. Polok [ap], P. Poropat [p], P. Privitera [ℓ], A. Pullia [r], J. Pyyhtia [af], D. Radojicic [s], S. Ragazzi [r], P.N. Ratoff [s], A.L. Read [ag], N.G. Redaelli [r], M. Regler [b], D. Reid [ac], P.B. Renton [s], L.K. Resvanis [j], F. Richard [o], M. Richardson [ac], J. Ridky [f], G. Rinaudo [aa], I. Roditi [i], A. Romero [aa], I. Roncagliolo [u], P. Ronchese [ae], C. Ronnqvist [af], E.I. Rosenberg [ak], U. Rossi [aj], E. Rosso [i], P. Roudeau [o], T. Rovelli [aj], W. Ruckstuhl [ab], V. Ruhlmann [c], A. Ruiz [ah], K. Rybicki [ap], H. Saarikko [af], Y. Sacquin [c], J. Salt [g], E. Sanchez [g], J. Sanchez [aℓ], M. Sannino [u], M. Schaeffer [y], S. Schael [ℓ], H. Schneider [ℓ], M.A.E. Schyns [i], F. Scuri [p], A.M. Segar [s], R. Sekulin [d], M. Sessa [p], G. Sette [u], R. Seufert [ℓ], R.C. Shellard [a], P. Siegrist [c], S. Simonetti [u], F. Simonetto [ae], A.N. Sissakian [f], T.B. Skaali [ag], G. Skjevling [ag], G. Smadja [k,c], G.R. Smith [d], N. Smirnov [w], R. Sosnowski [an], T.S. Spassoff [f], E. Spiriti [q], S. Squarcia [u], H. Staeck [t], C. Stanescu [q], G. Stavropoulos [x], F. Stichelbaut [z], A. Stocchi [o], J. Strauss [b], R. Strub [y], C.J. Stubenrauch [i], M. Szczekowski [an], M. Szeptycka [an], P. Szymanski [an], T. Tabarelli [r], S. Tavernier [z], G.E. Theodosiou [x], A. Tilquin [aq], J. Timmermans [ab], V.G. Timofeev [f], L.G. Tkatchev [f], T. Todorov [f], D.Z. Toet [ab], L. Tortora [q], M.T. Trainor [s], D. Treille [i], U. Trevisan [u], W. Trischuk [i], G. Tristram [v], C. Troncon [r], A. Tsirou [i], E.N. Tsyganov [f], M. Turala [ap], R. Turchetta [y], M.-L. Turluer [c], T. Tuuva [af], I.A. Tyapkin [f], M. Tyndel [d], S. Tzamarias [i], B. Ueberschaer [t], S. Ueberschaer [t], O. Ullaland [i], V.A. Uvarov [w], G. Valenti [aj], E. Vallazza [aa], J.A. Valls Ferrer [g], G.W. Van Apeldoorn [ab], P. Van Dam [ab], W.K. Van Doninck [z], N. Van Eijndhoven [i], C. Vander Velde [z], J. Varela [a], P. Vaz [a], G. Vegni [r], L. Ventura [ae], W. Venus [d], F. Verbeure [z], L.S. Vertogradov [f], L. Vibert [n], D. Vilanova [c], E.V. Vlasov [w], A.S. Vodopyanov [f], M. Vollmer [t], S. Volponi [aj], G. Voulgaris [j], M. Voutilainen [af], V. Vrba [q], H. Wahlen [t], C. Walck [m], F. Waldner [p], M. Wayne [ak], P. Weilhammer [i], J. Werner [t], A.M. Wetherell [i], J.H. Wickens [z], J. Wikne [ag], G.R. Wilkinson [s], W.S.C. Williams [s], M. Winter [y], D. Wormald [ag], G. Wormser [o], K. Woschnagg [ad], N. Yamdagni [m], P. Yepes [i], A. Zaitsev [w], A. Zalewska [ap], P. Zalewski [an], D. Zavrtanik [i], E. Zevgolatakos [x], G. Zhang [t], N.I. Zimin [f], M. Zito [c], R. Zitoun [n], R. Zukanovich Funchal [v], G. Zumerle [ae] and J. Zuniga [g]

[a] *LIP, Av. Elias Garcia 14 - 1e, P-1000 Lisbon Codex, Portugal*
[b] *Institut für Hochenergiephysik, Österreichische Akademie der Wissenschaften, Nikolsdorfergasse 18, A-1050 Vienna, Austria*
[c] *DPhPE, CEN–Saclay, F-91191 Gif-Sur-Yvette Cedex, France*
[d] *Rutherford Appleton Laboratory, Chilton, Didcot OX11 0QX, UK*
[e] *Department of Physics, University of Lund, Sölvegatan 14, S-22363 Lund, Sweden*
[f] *Joint Institute for Nuclear Research, Dubna, Head Post Office, P.O. Box 79, SU-101 000 Moscow, USSR*
[g] *Instituto de Fisica Corpuscular (IFIC), Centro Mixto Universidad de Valencia–CSIC, Avda. Dr. Moliner 50, E-46100 Burjassot (Valencia), Spain*
[h] *Department of Physics, University of Bergen, Allégaten 55, N-5007 Bergen, Norway*
[i] *CERN, CH-1211 Geneva 23, Switzerland*
[j] *Physics Laboratory, University of Athens, Solonos Street 104, GR-10680 Athens, Greece*
[k] *Université Claude Bernard de Lyon, 43 Bd du 11 Novembre 1918, F-69622 Villeurbanne Cedex, France*
[l] *Institut für Experimentelle Kernphysik, Universität Karlsruhe, Postfach 6980, W-7500 Karlsruhe 1, FRG*
[m] *Institute of Physics, University of Stockholm, Vanadisvägen 9, S-113 46 Stockholm, Sweden*
[n] *LPNHE, Universités Paris VI et VII, Tour 33 (RdC), 4 place Jussieu, F-75230 Paris Cedex 05, France*
[o] *Laboratoire de l'Accélérateur Linéaire, Université de Paris-Sud, Bâtiment 200, F-91405 Orsay, France*
[p] *Dipartimento di Fisica, Università di Trieste and INFN, Via A. Valerio 2, I-34127 Trieste, Italy and Istituto di Fisica, Università di Udine, Via Larga 36, I-33100 Udine, Italy*
[q] *Istituto Superiore di Sanità, Istituto Nazionale di Fisica Nucleare (INFN), Viale Regina Elena 299, I-00161 Rome, Italy*
[r] *Dipartimento di Fisica, Università di Milano and INFN, Via Celoria 16, I-20133 Milan, Italy*
[s] *Nuclear Physics Laboratory, University of Oxford, Keble Road, Oxford OX1 3RH, UK*
[t] *Fachbereich Physik, University of Wuppertal, Pf. 100 127, W-5600 Wuppertal 1, FRG*
[u] *Dipartimento di Fisica, Università di Genova and INFN, Via Dodecaneso 33, I-16146 Genoa, Italy*
[v] *Laboratoire de Physique Corpusculaire, Collège de France, 11 place M. Berthelot, F-75231 Paris Cedex 5, France*
[w] *Institute for High Energy Physics, Serpukhov, P.O. Box 35, SU-142 284 Protvino (Moscow Region), USSR*
[x] *Institute of Nuclear Physics, N.C.S.R. Demokritos, P.O. Box 60228, GR-15310 Athens, Greece*
[y] *Division des Hautes Energies, CRN–Groupe DELPHI and LEPSI, B.P. 20 CRO, F-67037 Strasbourg Cedex, France*
[z] *Physics Department, Universitaire Instelling Antwerpen, Universiteitsplein 1, B-2610 Wilrijk, Belgium and IIHE, ULB–VUB, Pleinlaan 2, B-1050 Brussels, Belgium and Service de Physique des Particules Elémentaires, Faculté des Sciences, Université de l'Etat Mons, Av. Maistriau 19, B-7000 Mons, Belgium*
[aa] *Dipartimento di Fisica Sperimentale, Università di Torino and INFN, Via P. Giuria 1, I-10125 Turin, Italy*
[ab] *NIKHEF-H, Postbus 41882, NL-1009 DB Amsterdam, The Netherlands*
[ac] *Department of Physics, University of Liverpool, P.O. Box 147, Liverpool L69 3BX, UK*
[ad] *Department of Radiation Sciences, University of Uppsala, P.O. Box 535, S-751 21 Uppsala, Sweden*
[ae] *Dipartimento di Fisica, Università di Padova and INFN, Via Marzolo 8, I-35131 Padua, Italy*
[af] *Research Institute for High Energy Physics, University of Helsinki, Siltavuorenpenger 20 C, SF-00170 Helsinki 17, Finland*
[ag] *Physics Department, University of Oslo, Blindern, N-1000 Oslo 3, Norway*
[ah] *Facultad de Ciencias, Universidad de Santander, av. de los Castros, E-39005 Santander, Spain*
[ai] *Dipartimento di Fisica, Università di Roma II and INFN, Tor Vergata, I-00173 Rome, Italy*
[aj] *Dipartimento di Fisica, Università di Bologna and INFN, Via Irnerio 46, I-40126 Bologna, Italy*
[ak] *Ames Laboratory and Department of Physics, Iowa State University, Ames IA 50011, USA*
[al] *Departamento de Fisica Atomica Molecular y Nuclear, Universidad Complutense, Avda. Complutense s/n, E-28040 Madrid, Spain*
[am] *Niels Bohr Institute, Blegdamsvej 17, DK-2100 Copenhagen Ø, Denmark*
[an] *Institute for Nuclear Studies, and University of Warsaw, Ul. Hoża 69, PL-00681 Warsaw, Poland*
[ao] *Physics Department, National Technical University, Zografou Campus, GR-15773 Athens, Greece*
[ap] *High Energy Physics Laboratory, Institute of Nuclear Physics, Ul. Kawiory 26 a, PL-30055 Cracow 30, Poland*
[aq] *Faculté des Sciences de Luminy, Université d'Aix – Marseille II Case 907 – 70, route Léon Lachamp, F-13288 Marseille Cedex 09, France*

Received 30 July 1991

The lifetime of the tau lepton has been measured by two independent methods using a silicon microvertex detector installed in the DELPHI detector. The signed impact parameter distribution of the one prong decays yielded a lifetime of $\tau_\tau = 321 \pm 36$ (stat.) $\pm$ 16 (syst.) fs, while the decay length distribution of three prong decays gave the result $\tau_\tau = 310 \pm 31$ (stat.) $\pm$ 9 (syst.) fs. The final value of the combined result was $\tau_\tau = 314 \pm 25$ fs. The ratio of the Fermi coupling constant from tau decay relative to that from muon decay was found to be 0.95 ± 0.04, compatible with the hypothesis of lepton universality.

1. Introduction

The tau lepton is a fundamental constitutent of the standard model and its lifetime is an important quantity which can be used to test the predictions of the model. In particular, the property of lepton universality can be tested using the relationship

$$\tau_\tau = \tau_\mu \left(\frac{G_\mu}{G_\tau}\right)^2 \left(\frac{m_\mu}{m_\tau}\right)^5 \mathrm{BR}\left(\tau^- \to \mathrm{e}^- \bar{\nu}_\mathrm{e} \nu_\tau\right), \qquad (1)$$

where $\tau_{\mu,\tau}$ and $m_{\mu,\tau}$ are the lifetimes and masses of the muon and tau respectively and $G_{\mu,\tau}$ are the Fermi constants determined from muon and tau decay [1].

The lifetime measurements presented in this paper were derived from the data taken by the DELPHI experiment at LEP during 1990. The $\tau^+\tau^-$ decay channel of the Z^0 boson was selected with a similar technique to that used for the published linescan [2]. Use was made of the precise $r\phi$ resolution of the silicon microvertex detector installed in the experiment in March 1990.

Two independent techniques were used to measure the lifetime. The first method was applied to taus which decayed to produce single charged particles. In this case, the lifetime was extracted from a measurement of the distance of closest approach of the decay particle trajectory to the Z^0 decay vertex, referred to as the impact parameter. In the second method, the decay vertex was reconstructed for those taus which decayed to produce three charged particles whose tracks were observed in the microvertex detector. As the interaction region of the LEP beams was small compared to the decay length, the production point of the taus could be taken as its centre, allowing the decay length to be determined and the lifetime calculated.

The DELPHI detector has been described in ref. [3]. In this analysis, the DELPHI charged particle tracking system in the polar angle range $43° < \theta < 137°$ was used. This consisted of four detectors:
the microvertex detector which is discussed in more detail in section 2;
the inner detector. This is a gas detector with a jet-chamber geometry. It produces 24 points per track, each with an $r\phi$ resolution of 90 μm;
the time projection chamber (TPC). This is the main tracking detector of DELPHI, situated between radii of 30 cm and 120 cm. It produces 16 points per track with an $r\phi$ resolution of 250 μm;
the outer detector. This consists of 24 modules containing 5 layers of drift tubes operating in limited streamer mode and situated at a radius of 2 m. A typical charged particle produces 5 points of 110 μm precision in $r\phi$.

Sections 3 and 4 describe the impact parameter and vertex analyses respectively, while section 5 presents the combined result of the two independent measurements and the conclusions.

2. The microvertex detector

The DELPHI microvertex detector [4] used in the present analysis consists of two concentric layers of silicon-strip detectors at radii of 9 and 11 cm respectively, giving full azimuthal coverage in the polar angle region $43^o < \theta < 137^o$. Each layer has 24 sectors with a 10% overlap in ϕ. A sector is subdivided along the beam direction into 4 silicon strip detectors (fig. 1). The silicon-strips are parallel to the beam direction and have a pitch of 25 μm with every second strip read out by capacitive pick-up. With this geometry an intrinsic resolution in the $r\phi$ plane of 7 μm can be obtained using charge division. The relative alignment of the modules was surveyed to an accuracy of 20 μm in three dimensions before installation in DELPHI. Movement relative to the rest of the DELPHI detector was monitored using lasers and capacitive sensors and found to be less than 5 μm over the running period.

[1] Permanent address: Département de Physique, Faculté des Sciences d'Oujda, Oujda, Morocco.

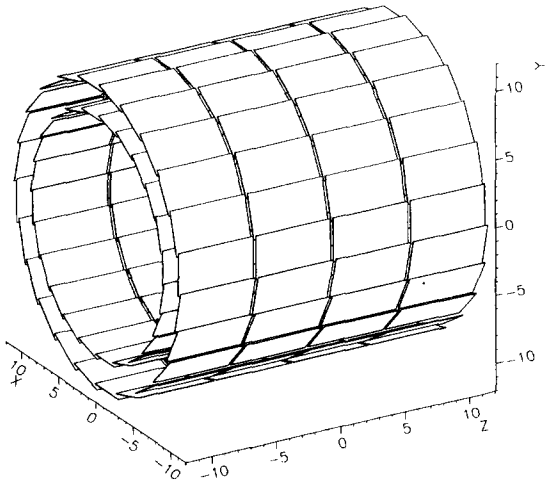

Fig. 1. Diagram of the microvertex detector, showing the two concentric layers of silicon strip detectors arranged in 24 ϕ sectors. Axis units are in centimetres.

To achieve the optimal spatial resolution in the experimental reference frame the final alignment was carried out using the dimuon decay channel of the Z^0, selected as described in ref. [2]. For the first half of the event sample collected in 1990, the two track elements for the muons in the outer detector were used to define a circle with a radius obtained from the momentum known from the beam energy. This was used to obtain the global alignment of the microvertex detector relative to the DELPHI coordinate system. The alignment of the corresponding sectors in the two layers relative to one another was then improved by a least squares circle fit to the microvertex detector hits alone.

The second half of the sample provided a check on the alignment using the distance of closest approach of the two muons in the $Z^0 \rightarrow \mu^+\mu^-$ sample, referred to as the muon miss distance, which is insensitive to the position of the interaction vertex. The two samples gave consistent results. The muon miss distance, calculated using only the hits from the two layers of the microvertex detector, had a standard deviation of 113 μm, corresponding to a track extrapolation resolution at the vertex $\sigma_{\text{ext}} = 113\ \mu\text{m}/\sqrt{2} = 80\ \mu\text{m}$. The resolution of the microvertex detector σ_{VD} can be related to σ_{ext} by the equation

$$\sigma_{\text{VD}}^2 = \frac{(r_2 - r_1)^2}{r_2^2 + r_1^2}\sigma_{\text{ext}}^2,$$

where r_1 and r_2 are the radii of the inner and outer layers of the microvertex detector respectively. This implies a microvertex detector resolution of 11 μm which can be considered as made up of contributions of 7 μm from the intrinsic resolution and 5 μm the mechanical stability combined with 7 μm from the alignment procedure.

3. The impact parameter method

For taus decaying to produce a single charged particle, the signed impact parameter is the distance of closest approach of the extrapolated track to the production point in the $r\phi$ plane. The sign is taken as positive if the extrapolated track intersects the tau direction before the point of closest approach and as negative otherwise. If the geometry of the production and decay could be reconstructed perfectly, the impact parameter would always be positive. Because of resolution effects and uncertainties in the tau direction it can be negative but its statistical distribution retains sensitivity to the tau lifetime. The geometric impact parameter, used below in the calculation of the resolution function, differs in that its sign is defined as the sign of the vector cross-product of the projections on the $r\phi$ plane of the track unit vector and the vector from the beam spot to the point of closest approach. This distribution should be symmetric about zero.

As a measure of the tau direction required for the sign of the impact parameter, the thrust axis of the event was used. This was determined by maximising the quantity $\sum_i |p_i^{\parallel}|$, where $p_i^{\parallel}$ is the momentum component along the chosen axis, for charged particles only. Monte Carlo simulation showed that the difference between this axis and the tau direction was centered on zero with a standard deviation of about 1^o.

The production point of the taus was taken as the centre of the interaction region measured for each LEP fill by reconstructing the vertices of Z^0 decays to multihadrons. The effects of the finite interaction region

were accounted for using the measurements on the $Z^0 \rightarrow \mu^+\mu^-$ events as described below.

The lifetime was extracted from the signed impact parameter distribution using a maximum likelihood method. The probability distribution for the impact parameter was determined as a function of the tau lifetime as follows: an impact parameter distribution was generated assuming zero microvertex error and a point interaction region using Monte Carlo generated events in which the effects due to tau decay kinematics and experimental cuts for tau selection were included. In order to account for the smearing due to the finite beam interaction region and the microvertex detector resolution, this impact parameter distribution was convoluted with a resolution function obtained from the geometric impact parameter distribution of the $Z^0 \rightarrow \mu^+\mu^-$ events. Studies of the hadronic events showed that for $p_t > 5$ GeV/c with respect to the beam axis the width of the resolution function was insensitive to the momentum and hence that the effect of multiple scattering on the resolution function was negligible. With this cut, the resolution function measured using dimuons could be used for the tau events with negligible systematic effect on the measured lifetime. The geometric impact parameter distribution for muons from $\mu^+\mu^-$ events with the same microvertex detector selection criteria as for taus is shown in fig. 2, together with the fitted resolution function calculated from the sum of two gaussians of widths 188 μm and 95 μm with a scaling of 0.395 of the broad gaussian relative to the narrow gaussian.

For reconstruction in the microvertex detector, only events where both taus decayed into single charged particles were considered. This gave a sample of 1710 events. An accepted track required a hit in both layers of the microvertex detector within an azimuthal angle of 0.4° of the track extrapolated from the rest of the DELPHI tracking system, and no other hit within 2.0°. Only events with 15 hits or less in the whole microvertex detector were used. A total of 1020 tau decays satisfied these criteria. In addition, the acollinearity projected onto the $r\phi$ plane was required to be greater than 0.5° in order to prevent a bias towards positive lifetimes that can occur if the projection of the track and the thrust axis on the $r\phi$ plane are almost coincident. In order to use the resolution function from the dimuons as described above, tau decays in the accepted events were only considered if the p_t of the decay particle was greater than 5 GeV/c. The final data sample comprised 724 tau decays.

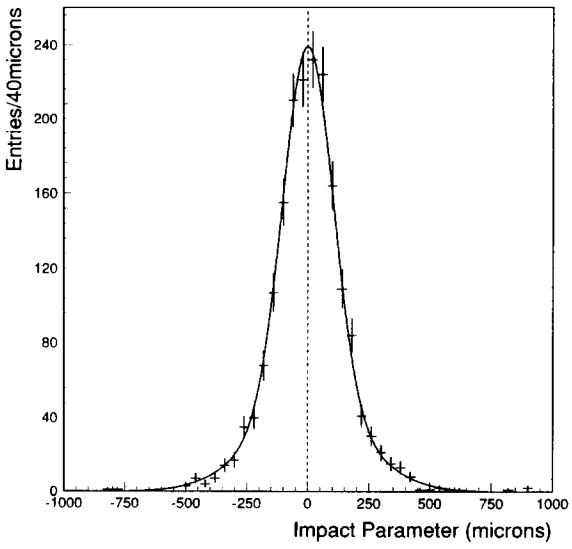

Fig. 2. The data points are the observed geometric impact parameter distribution for muons in $\mu^+\mu^-$ events. The curve is the best fit to a sum of two gaussians and was used as the resolution function in the impact parameter method.

The background contamination of the sample was determined from Monte Carlo to be 7.0±2.0%, mainly due to e^+e^- or $\mu^+\mu^-$ decays of the Z^0. A background contribution represented by the geometric resolution function from dimuons, suitably normalised and centred on zero, was included in the probability distribution.

The impact parameter was determined as the distance of closest approach between the centre of the interaction region and a circle through the two microvertex detector points with a radius calculated from the momentum measured using the rest of the DELPHI tracking system. Each decay was assigned a probability P_i using the probability function described above and the log likelihood, $\Sigma \ln(P_i)$, calculated as a function of the lifetime. The lifetime corresponding to the maximum value of the log likelihood was found to be 321 ± 36 fs. Fig. 3 shows the measured impact parameter distribution with the probability distribution calculated for this lifetime superimposed.

The analysis procedure was tested for bias by Monte Carlo simulation of tau decays with a known mean lifetime. This showed that systematic effects in the

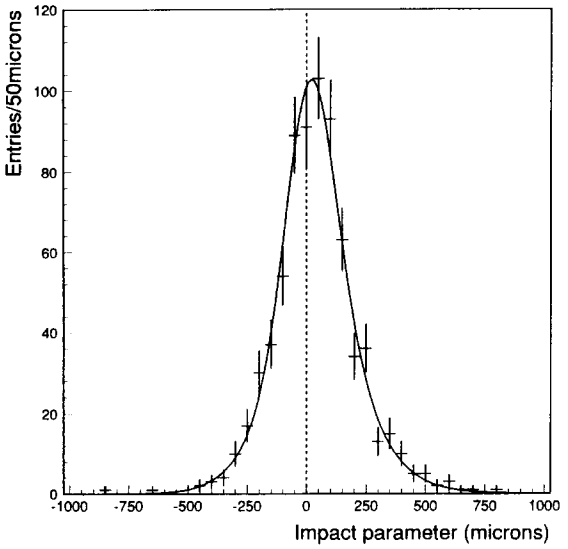

Fig. 3. The data points are the observed signed impact parameter distribution for taus. The curve shows the probability distribution for the fitted value of the tau lifetime, scaled to the number of tracks in the data sample.

analysis method were less than 3 fs. Systematic errors arose from: the uncertainty in the resolution function parameters due to the $Z^0 \to \mu^+\mu^-$ statistics where the errors in the parameterisation, including the correlations, were taken into account (14 fs); the uncertainty on the contamination in the sample of taus (7 fs); the uncertainty in the radial alignment of the microvertex detector (5 fs); the beam position (1 fs). Added in quadrature, these gave a total systematic error of 16 fs. As a further check on the consistency of the data, the lifetime has been calculated for positively and negatively charged decay particles, for two different ranges of ϕ and for positive and negative z. All values of the lifetime obtained were consistent with each other. The final result from the impact parameter method was:

$$\tau_\tau = 321 \pm 36 \text{ (stat.)} \pm 16 \text{ (syst.)} \text{ fs.}$$

4. The vertex method

In the sample of tau decays to three charged particles, the decay vertex can be reconstructed allowing a direct measurement of the the lifetime. In such events the other tau was required to decay to a single charged particle in order to minimise the background from hadronic decays of the Z^0. Monte Carlo studies showed that the background from hadronic and two-photon events was negligible in this topology. A total of 629 events were selected for the analysis.

The procedure for associating hits in the microvertex detector with tracks in the time projection chamber (TPC) began by defining a road in the $r\phi$ plane $\pm 15^o$ about the average ϕ of the three tracks seen in the TPC from the tau decay, corresponding to ± 29 mm at the outer layer of the microvertex detector. For the reconstruction of the tracks, at least 3 hits were required within the road in one layer of the microvertex detector and at least 2 hits in the other, giving a sample of 300 events.

For this sample circle fits to the first space point in the TPC and each hit in the outer layer of the microvertex detector, with the radius determined from the measured momentum, were extrapolated to the inner layer. The distribution of the residuals in the inner layer was found to agree with Monte Carlo calculations based on the resolutions of the TPC and a microvertex layer. All combinations with a hit in the inner layer within 100 μm were considered as possible associations. Acceptable combinations of associations for the three tracks had to use microvertex detector hits only once.

To reduce false sets of associations the additional constraint that the three tracks have to produce a good vertex was imposed. All tracks were first refitted using the TPC and both microvertex detector points. The decay vertex position (x,y) was estimated by minimising the function

$$\chi^2(x,y) = \sum_i \left(\frac{d_i}{\sigma_i}\right)^2,$$

where d_i is the distance of closest approach to the vertex in the $r\phi$ plane of particle i ($i = 1,2,3$). Correlations between the tracks were neglected. The error σ_i (in μm) was taken as

$$\sigma_i = \sqrt{\sigma_e^2 + \left(\frac{120}{p_i}\right)^2},$$

where σ_e is the extrapolation resolution for high momentum tracks, determined from the muon miss distance measured with the microvertex detector and

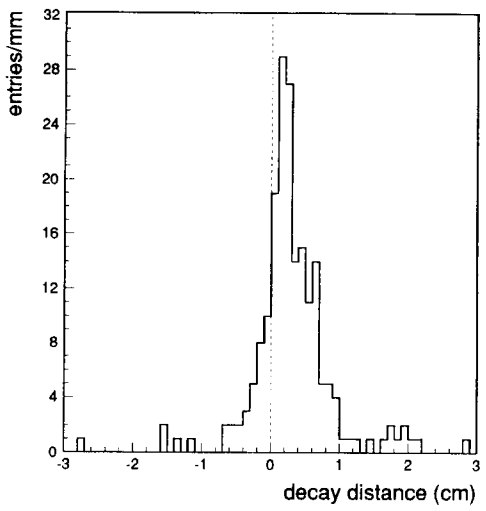

Fig. 4. The observed decay distance distribution for taus using the vertex method. The weighted mean decay length is 0.233 cm.

TPC, and has a value of 62 ± 3 μm. The second term is a parameterisation of the multiple scattering in the $r\phi$ plane due to the beam-pipe wall and the inner layer of the microvertex detector, where p_i is the transverse momentum in GeV/c of particle i.

An event was accepted if a vertex was reconstructed with a χ^2 probability greater than 0.01. Events with two or more accepted vertices were rejected unless the vertex error ellipses overlapped at the 2σ level. After these cuts, 148 three-prong decays remained. The χ^2 probability distribution of the accepted vertices was uniform, demonstrating that the tracking errors were well understood.

To determine the projected decay distance , d_i, the production point was taken to be the average centre of the interaction region during the 1990 data-taking. The laboratory decay distance, D_i, was calculated from

$$D_i = \frac{d_i}{\sin\theta_i},$$

where θ_i is the polar angle of the tau taken as that of the thrust axis of the three charged particles in the decay. The distribution of D_i is shown in fig. 4.

The decay time in the rest frame of the tau, T_i, is given by

$$T_i = \frac{D_i}{\beta\gamma c},$$

where $\gamma = (E/m_\tau)$ with E the average energy of the tau determined from the beam energy taking account of radiative corrections using KORALZ [5]. The lifetime was extracted from the distribution of decay times using the maximum likelihood method. The error in the decay time was assumed to come from a probability distribution with variance

$$\sigma_d^2 = \sigma_v^2 + \sigma_b^2,$$

where σ_v is the error on the reconstructed vertex projected along the thrust axis, typically 2 mm depending on the decay opening angle. The term σ_b accounts for the length of the interaction region along the thrust axis. Using the dimuons, it was found that the x and y projections of the interaction region averaged over the whole of the 1990 data-taking were well represented by gaussian distributions with $\sigma_x = 200$ μm and $\sigma_y = 80$ μm. These included the effects of beam size and movements of the beam centre during the data-taking period. For each event, the probability P_i of the event having a decay time T_i was calculated as a function of the lifetime τ using an exponential lifetime distribution convoluted with a gaussian distribution of width σ_d. The lifetime corresponding to the maximum of the log likelihood, $\Sigma \ln(P_i)$, was found to be 310±31 fs. The procedure was tested by analysing fully simulated events with five known lifetimes between zero and twice the world average. The results showed that the systematic effects associated with the analysis technique were less than 3 fs.

The systematic error arose chiefly from the uncertainty in the extrapolation resolution σ_e (8 fs). The systematic error arising from uncertainty in the association of the microvertex hits was estimated to be 4 fs by varying the size of the association region in the inner layer of the microvertex detector by 25 μm. Uncertainties in the beam position (2 fs), in the effect of inital and final state radiation (2 fs), in the determination of the tau direction (1 fs) and in the radial and azimuthal alignment of the microvertex detector (1 fs) have also been included. By adding all contributions in quadrature the total systematic error was estimated to be 9 fs.

Table 1
Recent measurements of the tau lifetime.

Tau lifetime (fs)	Experiment
$295 \pm 14 \pm 11$	ARGUS
$325 \pm 14 \pm 18$	CLEO
$299 \pm 15 \pm 10$	HRS
$309 \pm 17 \pm 7$	MAC
$288 \pm 16 \pm 17$	MARK II
$306 \pm 20 \pm 14$	TASSO
301 ± 29	JADE
$314 \pm 23 \pm 9$	This experiment

The final result of the vertex method was:

$\tau_\tau = 310 \pm 31$ (stat.) ± 9 (syst.) fs.

5. Summary and conclusions

The lifetime of the tau has been measured using two statistically independent methods, which agree well. Of the systematic errors, only those arising from the microvertex detector alignment and from uncertainty in the beam position are common to both analyses. Their contributions to the combined result were taken as the weighted mean of the corresponding uncertainties in the two methods. By combining the two results by weighting them with the reciprocal of the quadratic sum of the statistical and systematic errors a tau lifetime

$\tau_\tau = 314 \pm 23$ (stat.) ± 9 (syst.) fs,

is obtained. This result agrees with the value of 283 ± 7 fs predicted by eq. (1) using $\mathrm{BR}(\tau \to e\nu\nu) = 17.7 \pm 0.4\%$ [6]. Alternatively the measured lifetime may be used to determine the relative strengths of the Fermi coupling constants (G_τ/G_μ). This ratio is found to be 0.95 ± 0.04, consistent with lepton universality.

Table 1 shows a compilation of recent measurements of the tau lifetime [7]. The agreement among the measurements, including the one described here, is good.

Both methods are presently limited by statistics. For the 1991 LEP run, the microvertex detector has been upgraded by the addition of a third layer at a radius of 6 cm. This, together with an increased sample of events, will enable an improved measurement to be made.

Acknowledgement

We are greatly indebted to our technical staff and funding agencies for their support in building and operating the DELPHI detector, and to members of the SL division for the excellent performance of the LEP collider.

References

[1] Y.S.Tsai, Phys. Rev. D 4 (1971) 2821;
H.B. Thacker and J.J. Sakurai, Phys. Lett. B 36 (1971) 103.
[2] DELPHI Collab., P. Aarnio et al., Phys. Lett. B 241 (1990) 425.
[3] DELPHI Collab., Nucl. Instrum. Methods A 303 (1991) 233.
[4] H. Dijkstra et al., Nucl. Instrum. Methods A 289 (1990) 400;
V. Chabaud et al., Nucl. Instrum. Methods A 292 (1990) 75.
[5] S.Jadach and Z.Was, Comput. Phys. Commun. 36 (1985) 191;
S.Jadach et al., preprint CERN 89-08, Vol. 3 (1989) 67.
[6] Particle Data Group, Review of particle properties, J.J. Hernández et al., Phys. Lett. B 239 (1990).
[7] ARGUS Collab., H. Albrecht et al., Phys. Lett. B 199 (1987) 580;
CLEO Collab., C. Bebek et al., Phys. Rev. D 36 (1987) 690;
HRS Collab., M. Abachi et al., Phys. Rev. Lett. 59 (1987) 2519;
MAC Collab., H.R. Band et al., Phys. Rev. Lett. 59 (1987) 415;
MARK II Collab., D. Amidei et al., Phys. Rev. D 37 (1988) 1750;
TASSO Collab., W. Braunschweig et al., Z. Phys. C 39 (1988) 331;
JADE Collab., C. Kleinwort et al., Z. Phys. C 42 (1989) 7.